Heritage Science

RESEARCH

Open Access

Synergy of LIDAR and hyperspectral remote sensing: health status assessment of architectural heritage based on normal cloud theory and variable weight theory

Ming Guo[1,2,3], Xiaoke Shang[1], Jiawei Zhao[1,4*], Ming Huang[1,2,3], Ying Zhang[1,2,3] and Shuqiang Lv[1,2,3*]

Abstract

Architectural heritage health assessment is the basis of scientific repair and maintenance. However, existing methods do not adequately take into account the fuzziness, randomness and uncertainties unique to architectural heritage assessment. In this paper, a new evaluation model of VM-NCM is constructed by combining variable weight theory and normal cloud model theory. The model enables the combination of qualitative ratings and quantitative calculation, deals with the fuzziness in the assessment process, and resolves the randomness and reflects the uncertainty to a certain extent. Based on constructing the index system combining qualitative and quantitative indexes, the structural index values are acquired by the synergistic coupling of the fine laser point cloud model and finite element structural analysis model. The acquisition of surface index values is completed by the hyperspectral intelligent detection technology of surface materials and diseases. These reduce the generation of ambiguous information in the index detection process. An evaluation study is conducted using the Yingxian wooden pagoda in China as an example. The results show that this method takes into account the fuzziness and randomness in the evaluation process, and obtains more scientific and reliable evaluation results, which provides a research paradigm for assessing the architectural heritage health status.

Keywords Assessment index system, Synergy of LIDAR and hyperspectral remote sensing, Variable weight, Normal cloud model, Yingxian wooden pagoda

Introduction

The World Heritage Convention indicated that the protection and conservation of natural and cultural heritage were a significant contribution to sustainable development [1]. Natural disasters, environmental change, and human destruction accelerate the demise of cultural heritage. Among them, architectural heritage is immovable, non-renewable, and irreplaceable, so its preservation is urgent [2]. Although salvage reinforcement can maintain structural safety to some degree, it is impossible to restore the original aesthetic and historical value of damaged structural elements. It cannot fundamentally ensure the integrity of architectural heritage. Therefore, it is necessary to conduct a comprehensive assessment of the

*Correspondence:
Jiawei Zhao
zhaojiawei9921@163.com
Shuqiang Lv
lvshuqiang@bucea.edu.cn
[1] School of Geomatics and Urban Spatial Informatics, Beijing University of Civil Engineering and Architecture, Beijing 102616, China
[2] Engineering Research Center of Representative Building and Architectural Heritage Database Ministry of Education, Beijing 100044, China
[3] Beijing Key Laboratory for Architectural Heritage Fine Reconstruction & Health Monitoring, Beijing 102616, China
[4] China Oceanic Information Network, Tianjin, China

health status of architectural heritage [3]. It is an essential guide for the preventive conservation of architectural heritage and the realization of cultural preservation and sustainability.

Architectural heritage is a complex system with multiple coupled factors. There are three uncertainties in the process of assessing their health status: assessment index values, assessment criteria, and assessment results. In terms of evaluation index values, due to the limited inspection conditions and the requirements of cultural heritage protection, some complex structures cannot be fully inspected with instruments, or even if they can be inspected, there are problems with the accuracy of the equipment that lead to significant measurement errors. The variety and heterogeneity of surface diseases of architectural heritage cause fuzzy information to be generated. In terms of assessment criteria, the existing assessment norms are mainly qualitative in the description, and the classification of index levels lacks precise definition criteria and needs to be determined according to the actual severity of the assessment object, which inevitably causes the evaluation results to be influenced by the subjectivity of the inspectors, resulting in fuzziness. In terms of assessment results, the rating scale for a given indicator is judged by the inspector, which inevitably makes the assessment results random due to incomplete information and insufficient knowledge of the characteristics of the indicator. If the health status of architectural heritage is rated high, the existing problems will be overlooked, causing safety accidents and irreparable losses; on the contrary, it will lead to economic waste due to excessive reinforcement and preventive measures. The reason for this is the need for valid cognition of architectural heritage in multiple dimensions, perspectives and granularity, especially the lack of a comprehensive and practical assessment method that considers fuzziness, randomness and uncertainties.

The acquisition of assessment index values is divided into two aspects: structural parameters and surface parameters. In terms of structural parameter extraction: the contactless feature of LiDAR is used to obtain point cloud data for the 3D reconstruction of ancient buildings, which provides detailed and accurate engineering data for structural assessment of damaged ancient architectural heritage and strengthens the ability to perceive the safety state of buildings [4–8]. However, this cannot determine the force condition of the structure under external forces, which means that the spatial data model alone is insufficient to support the structural analysis of architectural heritage. The literature [9–12] used the finite element method to perform structural force analysis by approximating the solid structure with discrete grid cells. However, since the network models used are usually created in CAD software, they cannot be strictly considered "reality-based" 3D models and are not entirely consistent with natural objects, resulting in distorted results of FEM structural analysis. Therefore, the co-coupling of exemplary laser point cloud and FEA models is the primary trend and method to obtain more accurate quantitative calculation results. Regarding surface parameter extraction: there are various types of surface diseases of architectural heritage, and the categories of diseases also differ significantly. The extraction of diseases was mainly based on manual judgment in the early days, the method was time-consuming and laborious, and the recorded types of diseases and results needed to be more intuitive. Nowadays, digital technologies such as image processing, hyperspectral and 3D laser scanning are used to achieve semi-automatic or fully automatic extraction of diseases [13, 14]. Most of the pigment analysis of artifact surfaces using hyperspectroscopy utilizes linear mixed models in remote sensing, and fewer nonlinear mixed model studies have been conducted.

The problem of weighting the attributes of each indicator has become an essential issue in the study of the comprehensive multi-indicator evaluation process. The literature [15–20] uses the constant weight model (CWM) to determine the indicator weights. In this model, no matter how the state values change, the weights always remain the same and play a poor role in constraining the equilibrium of the grouping of target values. For example, in the condition assessment of the architectural heritage in this study, a very high score for a particular indicator represents a severe defect in the indicator, which affects the overall health degree. However, when the indicator's weight is small, this indicator with a high score tends to be neutralized, leading to an optimistic situation in the final evaluation results and reducing the reliability of the results. Therefore the overall assessment results calculated by CWM always imply that the architectural heritage is in good condition. This is because CWM suppresses the expressiveness of specific particular indicators, so these unique but potentially crucial indicators are not highlighted. To solve this problem, a variable-weight model that considers the relative importance of control factors is introduced to adjust the weights by responding to changes in the values of indicators [21–24].

The methods for modelling uncertainty in evaluating the health status of architectural heritage are based on cloud model theory (CM) with fuzzy sets. In the literature [25–28], when representing uncertainty in the evaluation process, fuzzy concepts are converted to exact values or intervals using fuzzy operators such as trapezoidal fuzzy numbers, thus losing part of the uncertainty in the conversion. It may still lead to unreliable

evaluation results. CM can quantify complex uncertainty through expectation, entropy, and superb entropy to achieve conversion between a specific qualitative concept and its quantitative representation. This maximally overcomes the randomness and subjectivity of fuzzy concepts and improves the credibility of evaluation results [29, 30]. Therefore, fuzzy set theory is less precise than CM in expressing uncertainty.

Research aim

This paper aims to address the effects of uncertain factors such as randomness and fuzziness in the evaluation of the architectural heritage health status. To this end, a zonal variable-weight model suitable for architectural heritage is proposed to solve the problem of unsatisfactory evaluation results due to too many indicators with constant weights, highlighting the adverse effects of indicators with higher risks so that more reasonable results can be obtained. The theory of Normal Cloud Model (NCM) is introduced into the comprehensive evaluation of this complex system, collaborating with the acceptable LiDAR point cloud model, finite element analysis model and hyperspectral quantitative inversion model for millimetre-level quantitative analysis, combined with expert wisdom using natural language descriptions for accounting for influencing factors such as natural weathering, structural deformation and material properties into the measurement information, forming a two-way cognitive calculation with the active participation of multiple parameters The process of multi-parameter active participation in the two-way cognitive calculation, through the calculation between NCMS to communicate the uncertainty better, so that it is more fully and accurately expressed. This provides a model for the two-way mapping of "quantitative description and qualitative concept" for the assessment of the architectural heritage health status.

Materials and methods

Construction of the evaluation model

Four-layer assessment index system

To construct an assessment index system that can describe the structure and surface information of architectural heritage, the selection of indexes should follow the principles of comprehension, dynamism, operability, and representativeness. According to the characteristics of architectural heritage, the assessment index system is divided into the target layer, criteria layer, index layer, and subsidiary layer. The overall health status of the architectural heritage is treated as the target layer. The foundation base, upper load-bearing structure, and containment system are divided into the criteria layer. Then, based on sub-units, the evaluation object is further refined as the evaluation index layer. Per the evaluation elements specified in the applicable criteria for the safety assessment of architectural heritage, the selected indices are further refined to obtain the subsidiary layer based on the structural and surface characteristics of the architectural heritage. The architectural heritage health assessment index system is shown in Fig. 1.

The structural residual damage and surface health of each component is evaluated from qualitative and quantitative viewpoints. A total of forty-five subsidiary indexes are divided. Among them, the appearance health index is primarily determined by the extent of discoloration, fading, smoke-dried, dust, mud and water stains, graffiti, and other ailments. The qualitative health index is primarily determined by the seriousness of efflorescence, salting, microorganisms, and other disorders. The quantitative index of surface health is mainly based on the deformation health index, which depends on the spatial shape changes of surface scratches, hollows, and shedding. The five evaluation indexes are disease damage index (DRI), density index (DI), boundary density index (BDI), fragmentation index (FI), and surface undulation index. The details are described in Appendix Table 4.

Method of obtaining indicator values

Structural health indicators for assessing deformation There are thirty-one structural health indicators in the assessment index system of architectural heritage health. It comprises seventeen qualitative assessment indicators, such as material, damage, node joint, etcetera, and fourteen quantitative assessment indicators, including settlement value, bearing capacity, tilts deformation, etcetera. Qualitative indicators are assessed based on expert scoring. Firstly, expert evaluation forms for qualitative indicators are designed. Secondly, qualitative indicator evaluation forms are distributed to experts with extensive research experience in specific architectural heritage, experts in the monitoring field, and experts in structural analysis. Furthermore finally, qualitative indicators were evaluated based on the feedback results from experts. Quantitative indicators are evaluated based on accurate measurement and analysis data based on the point cloud and finite element model regarding published high-level papers and other information.

Create a precise control network using measurement sensors like ground-based LiDAR and measurement robots. Precise monitoring data is gathered to capture alterations in architectural elements, acquiring a point cloud model with accurate coordinates. Next, the model is divided into many perspectives to examine the architectural legacy's distortion quantitatively. For example,

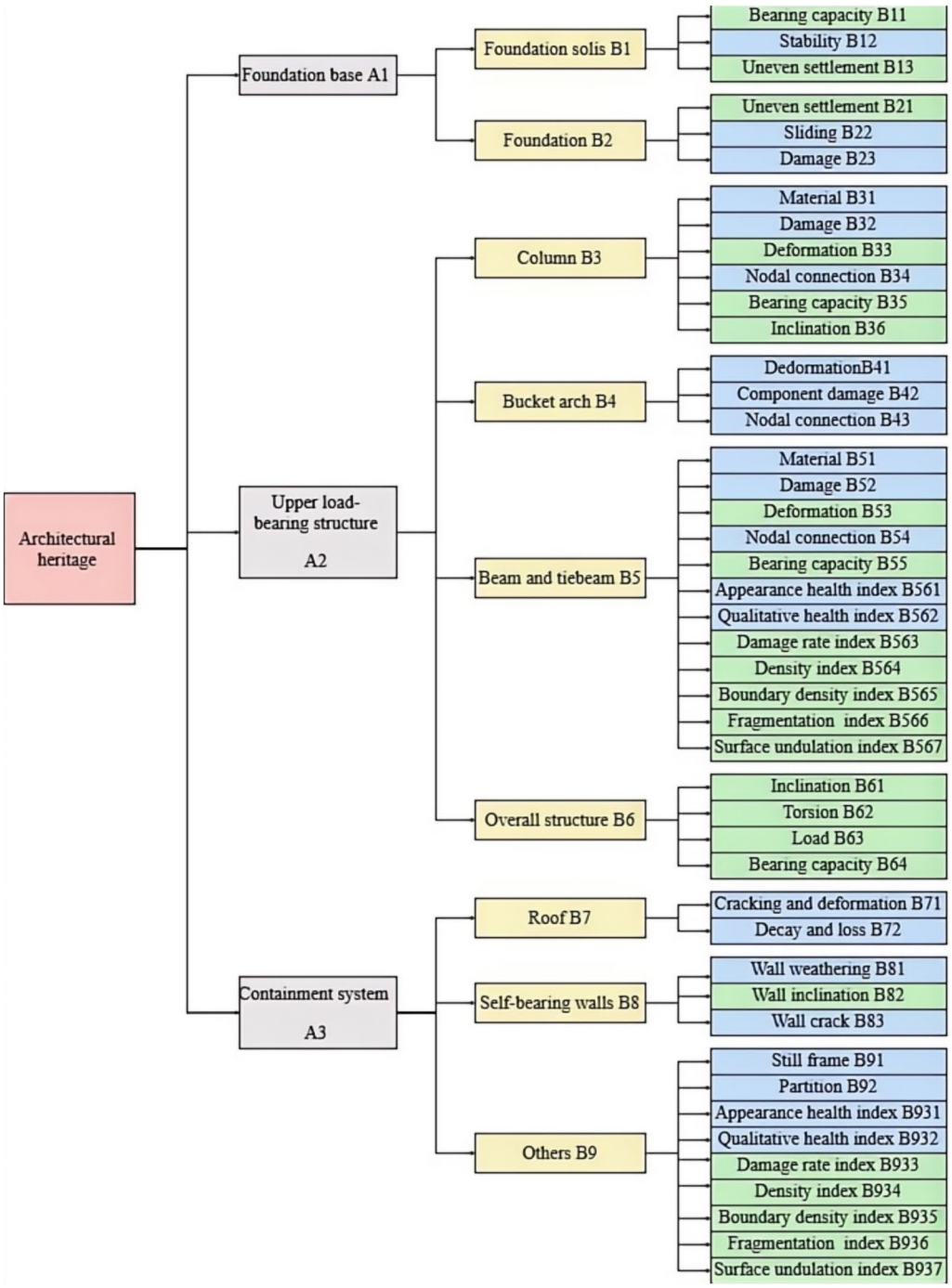

Fig. 1 Health assessment index system of architectural heritage: qualitative indicators are shown in blue, and quantitative in green

let's use the study and evaluation of the column structure Inclination (B36) index to illustrate: retrieve the column coordinates that share the same name from the two-phase point cloud. Subsequently, divide them along multiple axes to quantitatively assess individual and single-story columns' tilt angle and offset distance. This analysis will provide insights into the tilt condition of the column structure. As seen in Fig. 2. In the diagram, the transverse direction refers to the east–west direction, while the longitudinal direction refers to the north–south

direction. The integrated offset is the center distance between the column head and foot circle. The production of imprecise data is minimized during the non-destructive examination of architectural heritage elements.

Point cloud modeling is a valuable method for analyzing the deformation of architectural heritage. However, it does not take into account the examination of structural stress. Finite element analysis, however, can replicate the stress and strain behavior of an item when subjected to

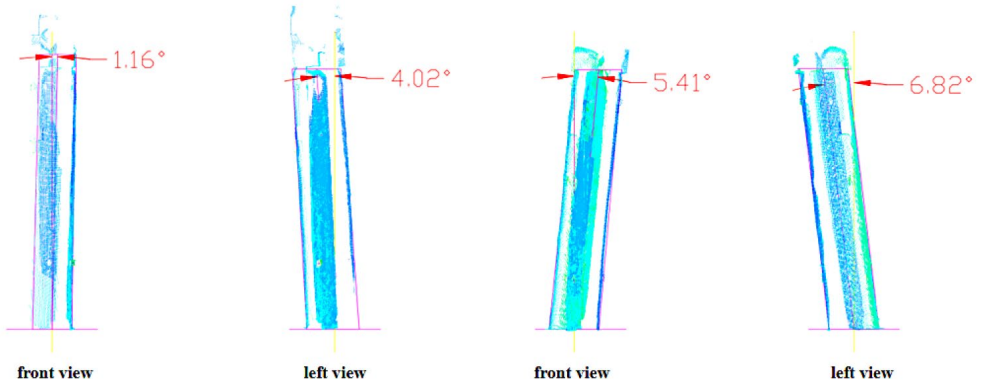

(a) Inclination angle of some columns (North-West and South-West)

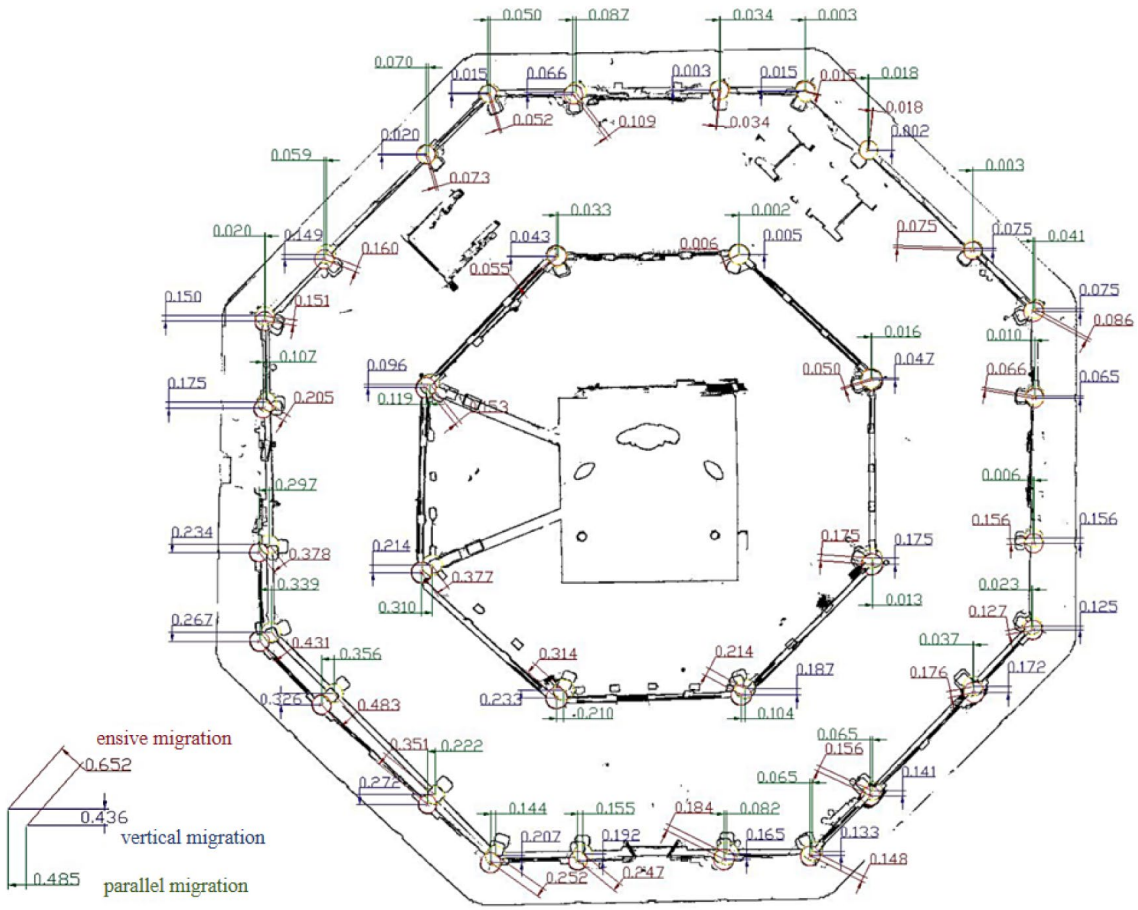

(b) Single-floor column offset

Fig. 2 Tilt of some columns

external forces. Nevertheless, as computer-aided design software typically produces the mesh model, precisely depicting the three-dimensional solid structure is imperative. Thus, a method that combines an acceptable laser point cloud model with a finite element structural analysis model is employed to create a dense point cloud for geometric analysis using finite element methods. This allows for calculating essential parameters such as bearing capacity and load. This article uses voxels as an intermediary to transform the chaotic and sparse point cloud data into a structured 3D pixel (voxel) arrangement, creating a hexahedral finite element mesh model. Every point is assigned to the corresponding voxel based on its coordinates, and any empty voxels are filled to ensure no gaps. The voxel model's external vertices are subsequently remapped to the original point cloud data to maintain the precise geometric characteristics of the model. A hexahedral mesh is created and then optimized. The final model file is divided into sections and reassembled to create the analytical model in Stp format. The output for finite element analysis is a hexahedral mesh with high-quality characteristics. This is demonstrated through the force analysis of the arch, as depicted in Fig. 3.

Spectral health indicators for assessing surface The surface health indicators in the architectural heritage health state assessment index system include four descriptive qualitative assessment indicators, such as the appearance health index, and ten quantitative assessment indicators for precise measurements, such as the degree of disease breakage. The analysis and evaluation of qualitative and quantitative indicators presuppose the identification of the surface materials of architectural heritage and the extraction of diseases, and the evaluation is based on the analysis results. Qualitative indicators are based on the severity of the disease. They are finally processed to form the appearance and qualitative health indexes using a graded qualitative evaluation method, as shown in Appendix Tables 5 and 6. Quantitative indexes were calculated and evaluated according to hyperspectral image disease extraction results. The specific calculation is shown in Appendix Table 4.

For the analysis of identifying individual pigments in materials, a method called spectral segmentation identification is used. This method takes into account the absorption features of ions to determine the types of pigments present on the surface of the fresco and to create a visual representation of the distribution of each pigment. Ion absorption features are spectral characteristics that indicate the presence of specific ions, such as iron, copper, manganese, etc., in a material. By using the absorption characteristics of these ions in spectrum analysis, it is possible to identify and differentiate pigments with similar visual spectral properties but varying chemical compositions more accurately. The picture is divided into a uniform zone based on the reflectance spectral values. Next, the spot spectra obtained from the homogeneous region are averaged to reduce the segmented homogeneous patch. These averaged spectra are then compared with the spectral library to determine the matching results for the pigments, as depicted in Fig. 4a. The enhanced Kubelka–Munk (KM) model was employed to reverse-engineer the composite pigments on the mural surface to identify and analyze such pigments. This model is a theoretical framework employed to describe the process of light absorption and scattering in non-transparent substances like pigments or paints. Initially, it is necessary to ascertain the absorption and scattering coefficients of each pigment present in the material. Subsequently, by utilizing these coefficients, determining the specific composition and quantity of each color inside the mixture can be achieved through inverse deduction. Figure 4c demonstrates identifying and quantifying pure pigments to determine their composition, quantity, fading pattern, weathering products, and mechanism.

The study focuses on analyzing the mural ground combat layer's spectral properties and the white pattern concerning disease extraction. The approach for

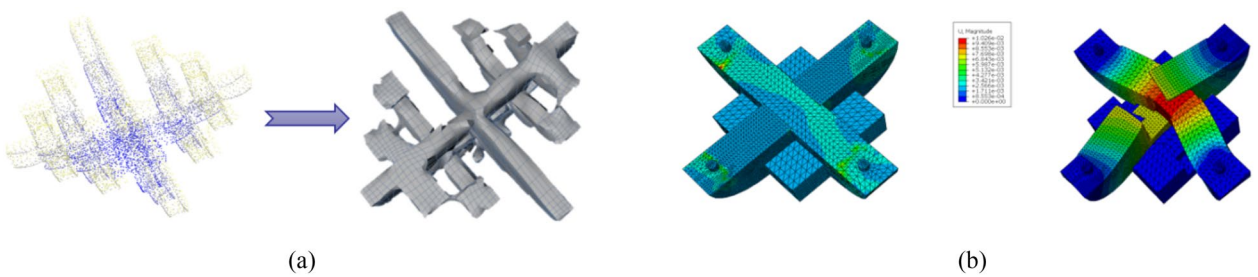

Fig. 3 The geometric analysis model of bucket arch point cloud is generated and the structural stress analysis is carried out: **a** dense point cloud generates finite element geometric analysis model; **b** stress analysis

Fig. 4 Segmented recognition results of single pigment spectrum considering ion absorption: **a** spatial distribution of four typical pigment homogeneous regions; **b** true color image; **c** improved K–M model and sparse demixing results (abundance maps of unmixed lithic green, cinnabar and lapis lazuli)

recognizing surface diseases in architectural heritage considers spectral and shape characteristics. A surface disease extraction method is employed to extract diseases such as scratches, hollowing, and shedding based on an enhanced U-net neural network. The shedding disease is identified by a technique that considers spectral and morphological characteristics, as depicted in Fig. 5a. Supervised classification using a Support Vector Machine (SVM) is utilized to extract and analyze Hu rectangle-like characteristics. This is done to identify and examine the critical shape difference between the pigment layer's peeling area and the white pattern's edge. The shape features are used to differentiate and extract the region of pigment layer shedding precisely, as well as the white pattern. The U-net network was enhanced by incorporating a spatial pyramid pooling layer in the encoding stage to retain the low-level features and utilizing a pooling index upsampling technique in the decoding stage to restore the image boundaries accurately. This improvement was made to develop a disease extraction model specifically designed for identifying the scratch disease, as depicted in Fig. 5b. Once the dataset has been trained, the model makes predictions. Then, a binarization post-processing technique is applied to the two test region murals to remove scratch lesions accurately.

Assigning constant weights to indicators through the combination weighting method

This research proposes a rational approach for giving weights to decision-making indicators by taking into account the intrinsic statistical laws and authoritative values associated with the indicator data. That is, it utilizes a blend of subjective and objective assignment techniques. Decision-makers can utilize this tool to modify the weights assigned to different factors in various scenarios. This allows them to flexibly select the most suitable weight ratios based on the specific circumstances. By doing so, they can balance subjective and objective weight values while eliminating any subjective bias or objective one-sidedness. The hierarchical analysis method (AHP) is frequently employed for subjective empowerment. It is particularly suitable for evaluation problems that involve the direct quantification of criteria or complex interrelationships between criteria. AHP allows for the utilization of experts' experience and judgment. The multifactorial and multilevel attributes of wood structures and historic edifices determine the pronunciation. The entropy weight approach used in objective assignment may effectively differentiate the information contribution among indicators, ensure a rational distribution of weights, and minimize the impact of subjective judgment. In contrast to objective assignment methods like PCA and factor analysis, the entropy weight method is more straightforward

Fig. 5 Extraction results of architectural heritage surface diseases: **a** the results obtained by the extraction method of shedding diseases based on the combination of spectrum and shape; **b** scratch extraction results based on improved U-Net

to calculate more accessible to implement. It prevents the potential loss of information that might occur with data dimensionality reduction. Hence, integrating AHP with the entropy weighting method enables the representation of decision-makers expertise and preferences, as well as the objective patterns within the data.

First, a survey on the significance of architectural heritage health assessment indicators and an objective weighing questionnaire is created to ascertain the subjective and objective weights. The significance and influence of the indicators are then evaluated by appropriate experts from historical sites, ancient structures, and research institutions.

Second, based on the questionnaire assignment findings, the judgment matrix for comparing evaluation indicators at the same level is built. Then, the maximum matrix eigenvalue is calculated. The weight vector of the matrix is computed using Eq. (1), and the average random consistency test is carried out. The indication importance assignment results align with the recognition if the test is passed; otherwise, it must be reassigned. Mean values were used to estimate the subjective weights of the indicators for the weighing results of various experts.

$$A_i = \sum_{m=1}^{m} a_{im};\ w_i = A_i \Big/ \left(\sum_{i=1}^{m} A_i \right), \tag{1}$$

where a_{im} = the importance degree of indicator i relative to m; w_i = the subjective weight of indicator i.

Then, based on the feedback results of the questionnaire, the judgment matrix of the index impact scores can be constructed after the normalization process. The information entropy of the evaluation matrix is computed using Eq. (2), and the objective weights of the evaluation indices are derived using Eq. (3).

$$e_j = -k \sum_{i=1}^{n} P_{ij} \ln \left(P_{ij} \right);\ k = 1/\ln (h), \tag{2}$$

$$w_j = \left(1 - e_j\right) \Big/ \left(\sum_{j=1}^{m} \left(1 - e_j\right) \right), \tag{3}$$

where $P_{ij} = B'_{ij} \Big/ \left(\sum_{i=1}^{h} B'_{ij} \right)$; B'_{hm} = the standardized index score value; $i = 1, 2, \cdots, h$; $j = 1, 2, \cdots, m$.

Finally, the subjective weights are integrated with the objective weights by multiplication, and the combined weights are calculated by Eq. (4).

$$w_i = w'_i w^*_i \Big/ \left(\sum_{i=1}^{m} w'_i w^*_i \right), \tag{4}$$

where w_i = comprehensive weight; w'_i = subjective weight; w^*_i = objective weight.

Health state assessment algorithm

Weight adjustment: zonal variable weight model

The core concept of the variable weight principle is that the weights adjust based on the variations in the indicator state vector, providing a more accurate representation of the influence of the associated indicator state change on the decision-making system. The weight vector for the variable is derived from the indicator constant weight vector, and the weight vector for the state variable is used to readjust the distribution of weights accurately. It results in a weight value consistent with the decision maker's attitude toward the decision. The variable weight function establishes the connection between the weight vector and the state vector. It adjusts the weights of each indicator according to the change of the corresponding comment value (i.e., the EX value of the comment cloud) to achieve a reasonable distribution of weights in the evaluation process. The variable weight vector is shown in Eq. (5), where S(X) is the state variable weight vector.

$$W_{(X)} = W * S(X) \Big/ \sum_{j=1}^{m} W_j S_j(X). \tag{5}$$

A high score on a single indicator in architectural heritage assessment may significantly reduce the overall condition. However, a low score on an indicator does not necessarily improve the overall condition of architectural heritage. Therefore, the assessment of the health status of architectural heritage contains only the incentive component in the penalty incentive. This paper's state variable weight vector adopts an exponential-type function. According to the characteristics of the deterioration law of architectural heritage components, the state variable weight vector is determined, and its elements are defined as

$$S_j(X) = \begin{cases} c, & X \in [0, A_1) \\ e^{\alpha(X-A_1)} + c - 1, & X \in [A_1, A_2) \\ e^{\beta(X-A_2)} + e^{\alpha(A_2-A_1)} + c - 2, & X \in [A_2, A_3) \\ e^{\gamma(X-A_3)} + e^{\beta(A_3-A_2)} + e^{\alpha(A_2-A_1)} + c - 3, & X \in [A_3, A_4] \end{cases}, \tag{6}$$

where c, α, β, γ are the weighting parameters, and A_i is the threshold of the variable weight interval.

$[0, A_1)$ is the no-punishment-no-incentive interval. When the indicator status value is in this range, it is neither punished nor motivated subjectively. $[A_1, A_2)$ is the initial excitation interval. In this interval, the excitation amplitude increases as the state value increases but is smaller than that of the strong excitation interval. $[A_2, A_3)$ is a strong incentive interval. The incentive magnitude

of this interval is smaller than the extra strong incentive interval. $[A_3, A_4]$ is an extra strong incentive interval. This interval has the greatest degree of incentive.

In the variable-weight evaluation, the values of the weighting parameters and variable-weight interval thresholds are determined about the specific study area. The value of the variable weight interval boundary A_i is defined by the indicator residual value definition. A_1, A_2, A_3, A_4 are 10, 30, 60, and 100, respectively. If $x \in [0, 10]$, the component is in a good state, corresponding to neither punishment nor incentive. As x increases, the incentive level gradually increases. That is, as the condition of the components deteriorates, the overall condition of the building heritage decreases at an increasing rate. It is necessary to determine the weighting parameters based on determining the threshold value of the variable weight interval. Firstly, an evaluation unit is selected to satisfy the constraint that the four index values in the evaluation unit are in different variable weight intervals, one index value is in the initial incentive interval, and the rest are in neither the penalty nor incentive interval. Then the ideal variable weights (w_1, w_2, w_3, w_4) of the four indicators located in different variable weight intervals that meet the actual situation and the evaluation preferences of the decision maker under the condition of the combination of the level of the group of state values are determined. The variable weights of the four factors constructed in the selected evaluation cell are the evaluation attitudes and preferences of the decision maker. Then the calculated constant weight values $\left(w_1^0, w_2^0, w_3^0, w_4^0, w_5^0\right)$ and the factor index values are used to find the weighting parameter values, and the relationship equation is obtained as follows.

$$\begin{cases} K_1 c = (K_2 c + 1)^{K_3} \\ K_1 = (w_1^0 - w_1^0(w_1 + w_2 + w_3 + w_4) - w_1\left(1 - \left(w_1^0 + w_2^0 + w_3^0 + w_4^0\right)\right) / \left(w_1 w_5^0\right) \\ K_2 = \left(w_2 * w_1^0 - w_1 * w_2^0\right) / \left(w_1 * w_2^0\right) \\ K_3 = (X_5 - A_1) / (X_2 - A_1) \end{cases}. \tag{7}$$

Uncertainty assessment: normal cloud model

Architectural heritage health is dynamic. The evaluation of the degree to which each evaluation index affects the condition of architectural heritage is subjective. Therefore, the evaluation procedure and outcomes are random and fuzzy. Normal cloud is a recently created evaluation approach that may integrate fuzziness and randomness, complete the uncertainty conversion between qualitative and quantitative ideas, and more objectively and scientifically reflect evaluation outcomes. Therefore, in this paper, the theory of normal cloud is applied to the architectural heritage health assessment process, and the variable weight-normal cloud assessment model (VM-NCM) is constructed.

Normal cloud model represents the knowledge of architectural heritage health status variables through three numerical characteristics: Expectation Ex, Entropy En, and Hyperentropy He. Ex is the expectation of the cloud distribution in the quantitative domain, which indicates the center of gravity of the cloud droplet. It is the most representative quantitative point of the state level. En is the range of quantitative cloud values that the fuzzy notion, which reflects the fuzzy degree of health status level boundaries, may tolerate; He is the thickness of the cloud, which reflects the discrete degree of the cloud, depending on the degree of entropy uncertainty, and reflects the randomness of the evaluation index of architectural heritage.

The steps for constructing the combination weighting—normal cloud evaluation model are as follows.

a. The three characteristic parameters of the criteria cloud model are calculated. The health status of architectural heritage is divided into four classes: healthy, sub-healthy, morbid, and severe morbid, and the expectation, entropy, and hyperentropy of each state interval are calculated as in Eq. (8).

$$Ex' = (X_{max} + X_{min})/2;\ En' = (X_{max} - X_{min})/6;\ He' = kEn', \tag{8}$$

where $k = 0.1$; X_{max}, X_{min} = the upper and lower limits of the interval.

b. The three characteristic parameters of the assessment cloud model are calculated. N experts are asked to evaluate each indicator for a particular project, and their ratings are aggregated according to Eq. (8) to create a cloud model for evaluating individual indicators. Individual indicator evaluation clouds are combined into a comprehensive evaluation cloud model based on the fusion algorithm of the cloud model Eq. (9).

$$Ex_i = (1/n)\sum_{j=1}^{n} X_{ij};\ En_i = \sqrt{(\pi/2)} \times (1/n)\sum_{j=1}^{n} \left|X_{ij} - Ex_i\right|;\ He_i = \sqrt{S^2 - En_i^2}, \tag{9}$$

$$Ex = \sum_{i=1}^{m} Ex_i \times w_i;\ En = \sqrt{\sum_{i=1}^{m} \left(En_i^2 \times w_i\right)};\ He = \sum_{i=1}^{m} (He_i \times w_i), \tag{10}$$

where X_{ij} = the rating result of the jth expert for the ith indication; S = the variance of the sample.

c. The levels are determined. Additionally, the shape of the various normal cloud models differs. The maximum membership principle determines the similarity between the comprehensive evaluation and standard cloud models. Equation (11) is used to perform the calculation, and the larger the value of u, the greater the similarity. The grading grade of the health status of architectural heritage corresponds to the greatest degree of affiliation.

$$u = \frac{1}{k} \sum_{i=1}^{k} e^{\frac{-\left(x_i - Ex'\right)^2}{2\left(En'\right)^2}}, \tag{11}$$

where k = the number of cloud drops; x_i = the i-th cloud drop.

Case study

Study subject

This study is based on Yingxian wooden pagoda, for example, analysis. The Yingxian wooden pagoda, also known as the Buddha Palace Temple Sakyamuni Pagoda, was built in 1056 A.D. It is the oldest surviving pure wooden structure in the world and was certified as the "world's tallest wooden pagoda" by Guinness World Records in September 2016. Structurally speaking, the whole tower does not use a nail, relying on the wooden components to bite each other mortise and tenon. Although the wooden tower, through the storm, strong earthquake, and shell bombardment, is still standing after a thousand years have not fallen, its surface and structure have also been severe damage by the wooden tower components' increased load. The second and third floors of the wooden pagoda (especially the second floor) tilted thoughtfully. Therefore, it is essential to assess the safety status of the Yingxian wooden pagoda.

Calculation of indicator weights

The parameter values $(c, \alpha, \beta, \gamma) = (0.302, 0.017, 0.009, 0.007)$ are obtained based on Eq. (6). The state-variable weight vector function constructed in this paper is shown in Eq. (12).

$$S_j(X) = \begin{cases} 0.302, & x \in [0, 10) \\ e^{0.017(X-10)} - 0.698, & x \in [10, 30) \\ e^{0.009(X-30)} - 0.293, & x \in [30, 60) \\ e^{0.007(X-60)} + 0.017, & x \in [60, 100] \end{cases}. \tag{12}$$

According to the above combined weighting method to obtain the constant weight of the evaluation indexes and the use of the zonal variable weight model to adjust the relative weights of the subsidiary indexes, the results are shown in Table 1.

Evaluation of normal cloud model

The applicable norms and standards classify the comprehensive evaluation criteria of architectural heritage health into four levels, i.e., R = {healthy, sub-healthy, morbid, and severe morbid}, and quantify them within the interval [0, 1]. The characteristic parameters of the criteria cloud model for each level are shown in Table 2. The quantitative analysis results of structural health and surface health evaluation indexes of the wooden pagoda and the qualitative evaluation results of experts are normalized, and the digital characteristics of the cloud model are processed. Combined with the weight calculation, the digital characteristics of the cloud model for comprehensive evaluation of each layer are obtained, as shown in Table 3. The similarities of the target layer, criterion layer, indicator layer, and subsidiary layer are calculated based on the standard cloud digital features and comprehensive evaluation of cloud digital features, as shown in Table 3. In accordance with the above digital characteristics, the cloud models are drawn in MATLAB as follows: standard cloud model in blue, foundation cloud model in green, upper load-bearing structure cloud model in yellow, containment system cloud model in purple, and comprehensive evaluation cloud model in red. The blue standard cloud model graphic depicts, from left to right, the healthy, sub-healthy, morbid, and severe morbid levels, as shown in Fig. 6.

Discussion

Safety analysis of architectural heritage

The health status of the Yingxian wooden pagoda has been analyzed using the established normal cloud model. The health levels of components, subunits, and evaluation objects were determined independently. The health state of each appraisal unit was analyzed specifically. The similarity calculation results are shown in Table 3, and the subunit and overall cloud models are shown in Fig. 6.

Foundation base. The overall rating of the foundation base (A1) is sub-healthy. The foundation soils (B1) and foundation (B2) are both sub-healthy. The bearing

Table 1 Constant and variable weights of evaluation variables

Criteria layer	Weight	Index layer	Weight	Subsidiary indexes	Constant weight	Variable weight	Subsidiary index	Constant weight	Variable weight	Subsidiary index	Constant weight	Variable weight
A1	0.487	B1	0.583	B11	0.391	0.502	B12	0.390	0.217	B13	0.219	0.281
		B2	0.417	B21	0.303	0.404	B22	0.373	0.233	B23	0.324	0.362
A2	0.462	B3	0.245	B31	0.043	0.033	B32	0.025	0.027	B33	0.051	0.039
				B34	0.170	0.125	B35	0.323	0.245	B36	0.388	0.532
		B4	0.127	B41	0.428	0.435	B42	0.109	0.112	B43	0.463	0.454
		B5	0.198	B51	0.252	0.169	B52	0.125	0.147	B53	0.114	0.151
				B54	0.152	0.146	B55	0.147	0.226	B561	0.033	0.02
				B562	0.033	0.020	B563	0.033	0.025	B564	0.012	0.009
				B565	0.033	0.029	B566	0.033	0.025	B567	0.033	0.032
		B6	0.43	B61	0.154	0.205	B62	0.189	0.175	B63	0.219	0.207
				B64	0.438	0.413						
A3	0.051	B7	0.387	B71	0.583	0.571	B72	0.417	0.429			
		B8	0.488	B81	0.314	0.390	B82	0.372	0.233	B83	0.314	0.377
		B9	0.125	B91	0.566	0.562	B92	0.154	0.154	B931	0.031	0.024
				B932	0.031	0.032	B933	0.031	0.032	B934	0.036	0.037
				B935	0.084	0.090	B936	0.031	0.032	B937	0.036	0.037

Table 2 Criteria cloud model digital features

S/N	Grade	Interval	Digital characteristics
A	Health	[0, 0.1)	(0.05, 0.017, 0.002)
B	Sub-health	[0.1, 0.3)	(0.20, 0.033, 0.003)
C	Morbid	[0.3, 0.6)	(0.45, 0.050, 0.005)
D	Severe morbid	[0.6, 1]	(0.80, 0.067, 0.006)

capacity (B11) and uneven settlement (B13) in foundation soils are sub-healthy while the stability (B12) is healthy. All three evaluation indicators (B21, B22, B23) in the foundation are sub-healthy. It is consistent with the actual measurement results in the field. The analysis of Fig. 6 shows that the foundation base is sub-healthy, which does not affect the overall bearing and can meet the normal use requirements. However, under long-term loading, its bearing capacity and other indicators cannot meet the normal use of the building. Therefore, it needs to be repaired and strengthened.

Upper load-bearing structure. The overall rating of the upper load-bearing structure (A2) is morbid. The columns (B3), beams and tiebeam (B5), bucket arche (B4), and overall structure (B6) included in them all belong to the third level of the standard cloud model with the largest affiliation. Only the hyperspectral indicators are mostly sub-healthy among the subsidiary layer indicators, while all others are morbid. The inclination (B36), deformation (B53) and bearing capacity (B55) of the beam and tiebeam, and the inclination (B61) of the overall structure are severe morbid. These indicators impact the overall load-bearing capacity. The indicator similarity corresponds to the actual scenario. Damage to structures, tilting, etcetera are the primary causes of morbid disorders. The upper load-bearing structures are all wooden components, which are more seriously damaged under the long-term natural environment and human factors, cannot meet the requirements of maintaining a healthy state, and are urgently needed to repair.

Containment system. The overall rating of the containment system (A3) is sub-healthy. Roofs (B7), self-bearing walls (B8), and others (B9) are all sub-healthy. The wall weathering (B81), boundary density index (B935), and Fragmentation index (B936) is morbid, and all others are in a sub-healthy state, which is consistent with the facts. Therefore, the wall and mural in the enclosure system must be repaired.

In terms of overall ratings, the evaluation grade of the Yingxian wooden pagoda is morbid. The upper load-bearing structure (A2) is more hazardous than the foundation base (A1) and containment system (A3). The damage and tilt of the local structure of the wooden pagoda have an enormous effect on the overall health. Consequently, local administration must be improved. The overall health status tends to become more morbid, consistent with the actual measured on-site condition. The results show that it is more scientific and reasonable to establish the normal cloud model for evaluating the health status of architectural heritage.

Reliability analysis of assessment results

The point clouds of the wooden pagoda for both phases were collected, as shown in Fig. 7a below, with the green points being the point cloud data for 2018 (the first phase) and the black points being the point cloud data for 2020 (the second phase). The data from the two periods are superimposed to analyze the changes in the column structure. Overall, it seems that the point clouds of the two periods overlap, and the wooden pagoda has no major deformation trend. From the cross-sectional point cloud in Fig. 7b, there is still tilt deformation between the column structures of the two phases.

Taking the second-story bright-story inner channel column as an example for detailed comparative analysis, the current state model of the inner channel column is shown in Fig. 8, with the column head inclined inward and the column foot inclined outward, showing a southwest to northeast stretch in the plane. Under the same measurement method of column structure offset, the measured offset of the slotted columns in both periods is shown in Fig. 9 below, the offset in 18 years is generally larger than that in 20 years, and the comparison of the point cloud data in both periods reflects the current situation and trend of deformation of the architectural heritage, which shows that the second bright floor of the architectural heritage with the most serious tilt is still continuously tilted, and the danger level of the architectural heritage is increasing, which is consistent with the assessment results.

Conclusions

This study uses architectural heritage as the research object, creates the assessment index system, and examines the health status of the Yingxian wooden pagoda in order to reach the following conclusions:

(1) For the first time, the structural deformation index and the spectral surface health index of architectural heritage are designed into the assessment index system to achieve the unification of the indexes. Under the existing related achievements, the assessment index system of the health status of architectural heritage consisting of 45 indicators is constructed from nine aspects: foundation soils, foundation, columns, bucket arches, beams and tiebeams, overall structure, roof, self-bearing walls,

Table 3 Evaluation clouds digital characteristics and their similarity to standard clouds

Index	Digital characteristics	Similarity				Index	Digital characteristics	Similarity			
		Healthy	Sub-healthy	Morbid	Serious morbid			Healthy	Sub-healthy	Morbid	Serious morbid
B11	(0.300, 0.042, 0.027)	9.57E−04	1.45E−01	9.27E−02	3.37E−07	B12	(0.103, 0.039, 0.011)	1.73E−01	1.12E−01	1.46E−06	2.01E−17
B13	(0.300, 0.042, 0.027)	2.26E−04	1.39E−01	8.66E−02	2.29E−07						
B21	(0.300, 0.042, 0.027)	4.26E−04	1.36E−01	8.15E−02	6.36E−06	B22	(0.117, 0.028, 0.008)	6.11E−02	1.21E−01	1.84E−07	4.78E−19
B23	(0.250, 0.125, 0.042)	3.42E−02	2.40E−01	1.13E−01	1.60E−03						
B31	(0.307, 0.078, 0.045)	5.60E−03	1.68E−01	1.73E−01	1.20E−03	B32	(0.583, 0.700, 0.031)	1.58E−02	4.49E−02	7.37E−02	8.83E−02
B33	(0.300, 0.042, 0.027)	1.30E−03	1.45E−01	8.92E−02	1.25E−06	B34	(0.290, 0.058, 0.030)	1.20E−03	1.86E−01	8.65E−02	7.64E−05
B35	(0.300, 0.042, 0.027)	8.50E−04	1.45E−01	8.55E−02	2.87E−06	B36	(0.933, 0.028, 0.008)	0	9.92E−78	3.14E−15	1.76E−01
B41	(0.550, 0.084, 0.023)	3.48E−24	1.70E−03	2.91E−01	4.34E−02	B42	(0.557, 0.114, 0.040)	9.52E−04	7.10E−03	2.66E−01	8.59E−02
B43	(0.520, 0.134, 0.037)	1.10E−03	1.86E−02	3.14E-01	7.29E−02						
B51	(0.217, 0.070, 0.031)	2.22E−02	4.75E−01	2.76E−02	3.73E−06	B52	(0.507, 0.078, 0.045)	2.09E−04	8.90E−03	4.81E−01	2.88E−02
B53	(0.617, 0.070, 0.031)	1.03E−39	6.44E−05	9.26E−02	1.24E−01	B54	(0.343, 0.070, 0.040)	3.20E-03	8.44E−02	2.80E−01	5.46E−04
B55	(0.833, 0.056, 0.015)	1.20E−224	8.66E−35	1.07E−05	7.13E−01	B561	(0.197, 0.011, 0.003)	4.25E−11	9.44E−01	5.27E−06	9.03E−18
B562	(0.197, 0.011, 0.003)	5.80E−10	9.44E−01	5.20E−06	8.93E−18	B563	(0.243, 0.014, 0.006)	4.24E−14	4.63E−01	4.33E−04	1.01E−14
B564	(0.240, 0.008, 0.005)	1.13E−18	6.03E−01	2.45E−04	1.84E−15	B565	(0.293, 0.022, 0.012)	1.06E−15	6.83E−02	2.15E−02	9.26E−11
B566	(0.250, 0.025, 0.008)	4.18E−10	3.78E−01	2.10E−03	1.25E−12	B567	(0.317, 0.028, 0.013)	2.56E−11	3.23E−02	6.80E−02	2.57E−09
B61	(0.633, 0.056, 0.015)	2.82E−100	1.22E−12	3.97E−02	1.26E−01	B62	(0.317, 0.070, 0.031)	1.70E−03	1.27E−01	1.59E−01	9.66E−05
B63	(0.333, 0.111, 0.030)	8.40E−03	1.37E−01	2.52E−01	1.40E−03	B64	(0.333, 0.028, 0.008)	4.67E−21	9.80E−03	1.14E−01	4.61E−09
B71	(0.140, 0.067, 0.018)	9.04E−02	3.18E−01	1.50E−03	9.45E−11	B72	(0.150, 0.042, 0.027)	5.35E−02	4.31E−01	9.34E−04	5.04E−12
B81	(0.307, 0.095, 0.026)	7.30E−03	1.74E−01	1.78E−01	2.81E−04	B82	(0.133, 0.028, 0.008)	2.49E−02	2.30E−01	5.20E−07	1.88E−18
B83	(0.293, 0.106, 0.042)	1.54E−02	1.97E−01	1.49E−01	2.30E−03						
B91	(0.290, 0.134, 0.038)	2.24E−02	1.90E−01	1.69E−01	3.40E−03	B92	(0.293, 0.011, 0.003)	3.39E−32	2.66E−02	9.20E−03	9.19E−13
B931	(0.220, 0.008, 0.005)	1.11E−14	9.61E−01	4.67E−05	1.76E−16	B932	(0.300, 0.025, 0.008)	1.26E−18	4.34E−02	2.80E−02	8.31E−11
B933	(0.300, 0.025, 0.008)	1.23E−17	4.59E−02	2.69E−02	6.45E−11	B934	(0.293, 0.022, 0.012)	5.80E−12	7.28E−02	2.05E−02	3.23E−11
B935	(0.337, 0.031, 0.010)	1.99E−25	9.70E−03	1.39E−01	7.51E−09	B936	(0.310, 0.008, 0.005)	1.05E−36	7.10E−03	2.68E−02	5.36E−12
B937	(0.297, 0.028, 0.013)	3.20E−13	7.62E−02	2.86E−02	1.24E−10						
B1	(0.223, 0.041, 0.021)	5.20E−03	6.04E−01	5.80E−03	3.28E−10	B2	(0.215, 0.077, 0.025)	2.62E−02	4.03E−01	2.39E−02	1.97E−05
B3	(0.551, 0.044, 0.021)	3.69E−67	5.44E−08	2.45E−01	1.25E−02	B4	(0.537, 0.112, 0.031)	3.22E−04	9.20E−03	3.16E−01	6.61E−02
B5	(0.415, 0.062, 0.027)	2.22E−04	1.21E−02	5.95E−01	5.95E−04	B6	(0.376, 0.066, 0.018)	5.06E−07	3.29E−02	3.91E−01	1.44E−04
B7	(0.144, 0.058, 0.022)	7.22E−02	3.34E−01	1.50E−03	2.57E−10	B8	(0.238, 0.081, 0.024)	1.59E−02	3.60E−01	4.71E−02	5.87E−06
B9	(0.291, 0.101, 0.024)	1.38E−02	2.04E−01	1.51E−01	4.16E−04						
A1	(0.220, 0.059, 0.023)	1.12E−02	4.97E−01	1.25E−02	3.34E−09	A2	(0.447, 0.069, 0.022)	1.66E−07	5.40E−03	6.07E−01	1.90E−03
A3	(0.208, 0.076, 0.023)										
	Target layer	(0.324, 0.065, 0.023)					5.5004e−04, 0.0969, 0.1785, 2.8240e−05				

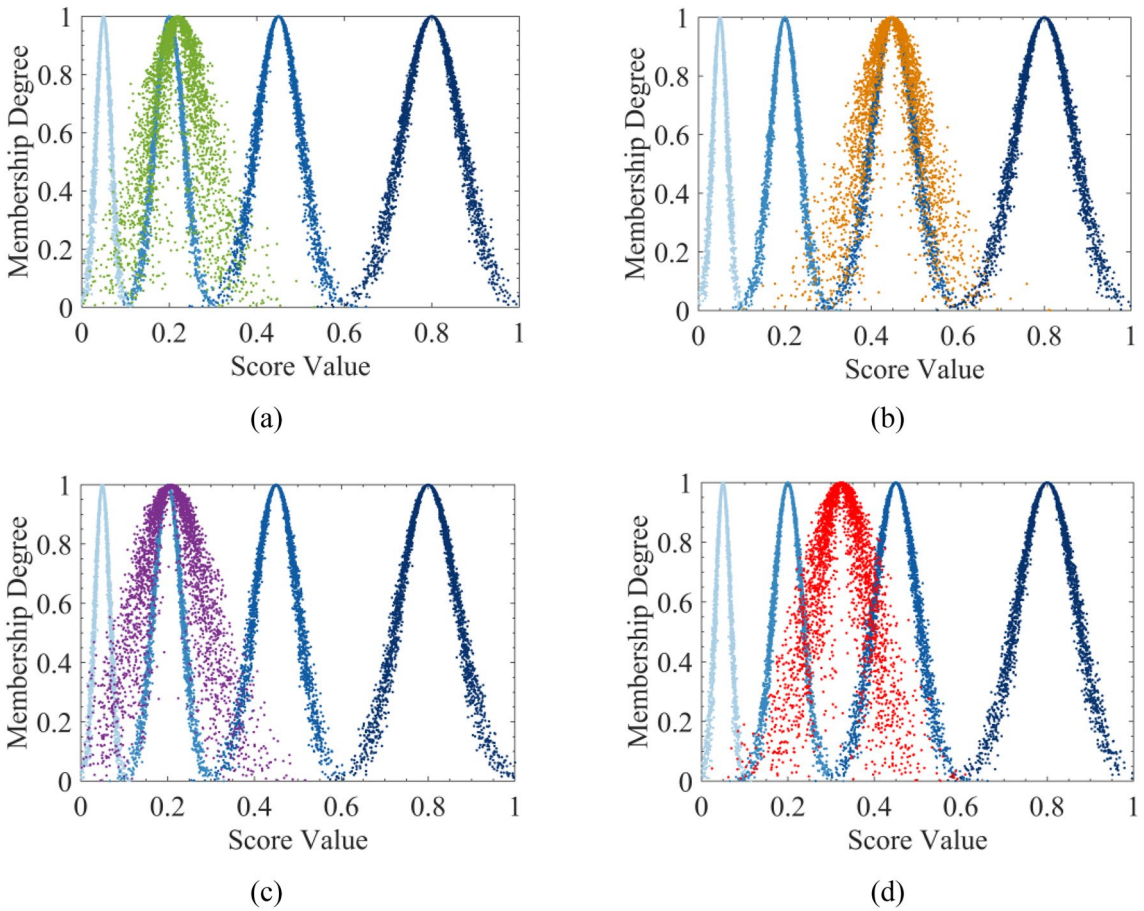

Fig. 6 The results of the assessment of the normal cloud model are, in order: **a** foundation base; **b** upper load-bearing structure; **c** containment system; **d** comprehensive assessment

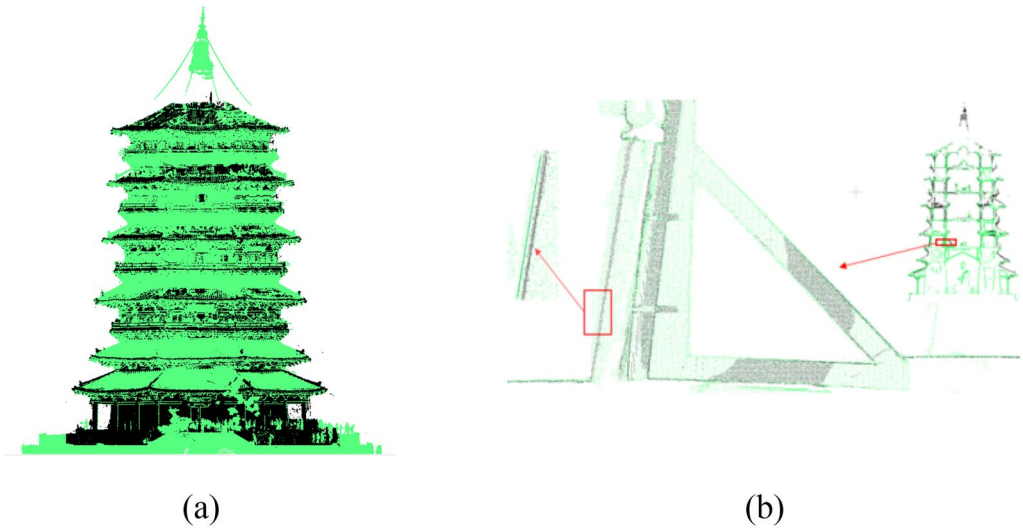

Fig. 7 Comparison of the point clouds of the two phases of architectural heritage: **a** overall point cloud **b** column cross-section

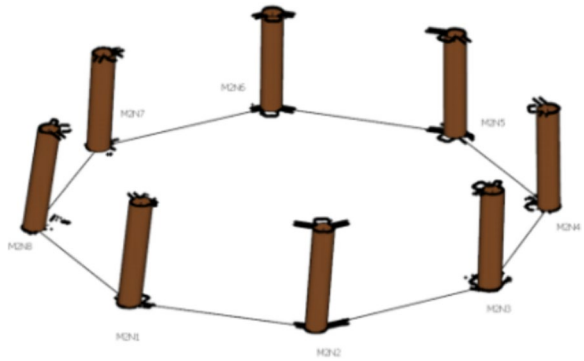

Fig. 8 Model of the second-story internal slot column

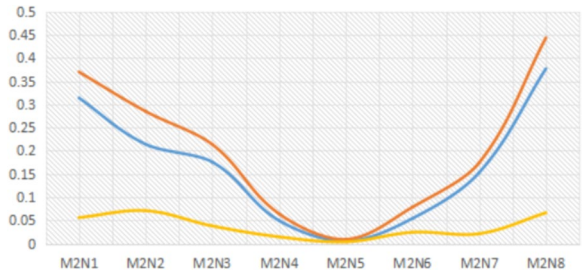

Fig. 9 Comparison of slot column offsets between two periods

and others, taking into account the structural health and surface health of architectural heritage. This system has four layers: target layer, criteria layer, index layer, and subsidiary layer.

(2) The problem of accurately quantifying architectural heritage's overall health index values has been solved. The structural index values are acquired by the synergistic coupling of the fine laser point cloud model and finite element structural analysis model. The acquisition of surface index values is completed by the hyperspectral intelligent detection technology of surface materials and diseases, which reduces the generation of ambiguous information in the index detection process. These provide technical support for architectural heritage health assessment.

(3) Establishing the evaluation model of VW-NCM. On the basis of the combination assignment weights, a zoning variable weight model suitable for architectural heritage is proposed to solve the problem of unsatisfactory evaluation effect caused by too many indicators with constant weights and highlight the negative effect of indicators with higher risk, so that more reasonable results can be obtained. The combination of variable weight theory and normal cloud model, considers the randomness and fuzziness in the evaluation process, realizes the uncertainty conversion between qualitative and quantitative, and improves the refinement level of architectural heritage health assessment.

(4) Since the assessment of the health status of architectural heritage involves multiple aspects and disciplines, the assessment results obtained through data analysis span a significant period. With the change of time, the index assessment results of the existing research data may be slightly different from the current situation of architectural heritage. Fundamental research for various fields of architectural heritage should be carried out in an orderly manner while carrying out fine mapping of architectural heritage and strengthening the damage to the complex components of architectural heritage. It is necessary to conduct a detailed mapping of architectural heritage and carry out basic research in various fields of architectural heritage in an orderly and strengthened understanding of the damage to complex components of architectural heritage.

Appendix

See Tables 4, 5, and 6.

Table 4 Health assessmenlet index system of architectural Heritage

Target layer	Criteria layer	Index layer	Subsidiary layer	Description
Architectural heritage	Foundation base A1	Foundation solis B1	Bearing capacity B11	Foundation soils bearing state
			Stability B12	Foundation soils stability
			Uneven settlement B13	Foundation soils settlement
		Foundation B2	Uneven settlement B21	Foundation settlement
			Sliding B22	Foundation sliding
			Damage B23	Damage such as foundation cracks or corrosion
	Upper load-bearing structure A2	Column B3	Material B31	The scope and extent of defects such as decay, insect infestation, aging and deterioration
			Damage B32	Damage to the column body due to fracture, splitting and external forces
			Deformation B33	The bending deformation evaluation index is the bending vector height δ1
			Nodal connection B34	The two ends of the connection, column foot and column base misalignment, column foot subsidence, etc.
			Bearing capacity B35	Load-bearing capacity of column structure
			Inclination B36	Column head and foot displacement
		Bucket arch B4	DedormationB41	Deformation and misalignment of bucket arch
			Component damage B42	Decay, indentation, splitting, fracture, and dislodgement of bucket arch
			Nodal connection B43	Compression or deformation or mutilation of tenon or mortise
		Beam and tiebeam B5	Material B51	The scope and extent of defects such as decay, insect infestation, aging and deterioration
			Damage B52	Cracking, non-original sawing, grooving and drilling
			Deformation B53	Deflection of beam square ω, lateral bending vector height δ1
			Nodal connection B54	Beam, square pluck tenon, broken tenon or split mortise
			Bearing capacity B55	Bearing capacity of beam and tiebeam
			Appearance health index B561	The surface of mural and color painting is not clear due to the fading of pigments
			Qualitative health index B562	Change of substance on the mural affects safety
			Damage rate index B563	The ratio of the area where the disease occurred to the overall area of the mural in which the experiment was conducted
			Density index B564	Number of diseases per unit area
			Boundary density index B565	Length of the border of the diseased plaque contained in the unit area
			Fragmentation index B566	The degree of fragmentation of mural paintings divided by disease
			Surface undulation index B567	Hollowing

Table 4 (continued)

Target layer	Criteria layer	Index layer	Subsidiary layer	Description
		Overall structure B6	Inclination B61	Overall tilt of load-bearing structures
			Torsion B62	Overall torsion of load-bearing structures
			Load B63	The overall load and its distribution
			Bearing capacity B64	Load capacity status
	Containment system A3	Roof B7	Cracking and deformation B71	Cracking
			Decay and loss B72	Leakage, collapse, decay and other quality defects
		Self-Bearing walls B8	Wall weathering B81	The degree of wall weathering
			Wall inclination B82	The degree of wall tilt
			Wall crack B83	
		Others B9	Still frame B91	Cracking, rotting, missing and so on
			Partition B92	Cracking, rotting, missing and so on
			Appearance health index B931	The surface of mural and color painting is not clear due to the fading of pigments
			Qualitative health index B932	Change of substance on the mural affects safety
			Damage rate index B933	The ratio of the area where the disease occurred to the overall area of the mural in which the experiment was conducted
			Density index B934	Number of diseases per unit area
			Boundary density index B935	Length of the border of the diseased plaque contained in the unit area
			Fragmentation index B936	The degree of fragmentation of mural paintings divided by disease

Table 5 Appearance health index evaluation form

	Score	The severity is normalized to [0, 1]
Discoloration	S1	P1
Fading	S2	P2
Smoke-dried	S3	P3
Dust	S4	P4
Mud and water stains	S5	P5
Graffiti	S6	P6
Weighted average	S	P

Good (> 80); better (80–70); average (60–70); severe (50–60); highly severe (< 60)

Table 6 Qualitative health index evaluation form

	Score	The severity is normalized to [0, 1]
Efflorescence	S1	H1
Salting	S2	H2
Microorganisms	S3	H3
Weighted average	S4	H

Good (> 80); better (80–70); average (60–70); severe (50–60); highly severe (< 60)

Acknowledgements
This research was supported by National Key Research and Development Program of China [Grant No. 2022YFF0904400, 2022YFF0904301]; National Natural Science Foundation of China [Grant No. 42171416].

Author contributions
Ming Guo: conceptualization, resources, supervision, funding acquisition. Xiaoke Shang and Jiawei Zhao: methodology, formal analysis, investigation, writing—original draft, writing—review and editing. Ming Huang: methodology, resources, supervision. Ying Zhang: validation, investigation. Shuqiang Lv: methodology, resources, supervision.

Data availability
Data will be made available on request.

Declarations

Consent for publication
The authors declare that this manuscript is original, has not been published before and is not currently being considered for publication elsewhere.

Competing interests
The authors declare that they have no known competing financial interests or personal relationships that could have appeared to influence the work reported in this paper.

Received: 29 April 2024 Accepted: 14 June 2024
Published online: 26 June 2024

References

1. UNESCO WHC. Policy document for the integration of a sustainable development perspective into the processes of the World Heritage Convention. Paris: General Assembly of States Parties to the World Heritage Convention at its 20th Session. 2015.
2. Sevieri G, Galasso C. Typhoon risk and climate-change impact assessment for cultural heritage asset roofs. Struct Saf. 2021;91: 102065.
3. Quagliarini E, Clini P, Ripanti M. Fast, low cost and safe methodology for the assessment of the state of conservation of historical buildings from 3D laser scanning: the case study of Santa Maria in Portonovo (Italy). J Cult Herit. 2017;24:175–83.
4. Guo M, Sun MX, Huang M, Yan BN, Zhou YQ, Zhao YS. High-precision measurement of steel structure based on LiDAR and UAV. Opt Precis Eng. 2021;29(05):989–98.
5. Wang G, Wu G, Wang Y, Guo M, Zhao J, Gao C. Deformation monitoring of ancient pagoda with multi-source data. Journal of Geo-information Science,20.2018 (2018): 496–504.
6. Guo M, Yan B, Zhou T, Pan D, Wang G. Accurate calibration of a self-developed vehicle-borne LiDAR scanning system. J Sens. 2021;2021(1):8816063.
7. Zhang X. The application of 3D laser scanning in the safety detection of ancient buildings. Bull Survey Map. 2020;1:155–8.
8. Guo M, Sun M, Pan D, Wang G. Zhou Y. Yan B. Fu Z. High-precision deformation analysis of yingxian wooden pagoda based on UAV image and terrestrial LiDAR point cloud. Heritage Science 11.1 (2023): 1.
9. Iraola B, Cabrero JM, Basterrechea-Arévalo M, Gracia J. A geometrically defined stiffness contact for finite element models of wood joints. Eng Struct. 2021;235: 112062.
10. Bukhari SM, Chandrasekaran R. Static and dynamic analysis of wood laminated composite poles using FEA. Mater Today Proc. 2019;19:843–9.
11. Barsanti SG, Guidi G. A new methodology for the structural analysis of 3D digitized cultural heritage through FEA. In: IOP conference series: materials science and engineering, vol. 364, No. 1. IOP Publishing; 2018.
12. Xue J, Wu C, Zhai L, Wang R, Ma L. Finite element analysis on seismic responses of Yingxian Wooden Tower by considering the effect of stylobate. J Civ Environ Eng. 2022;44(2):22–9.
13. Lv SQ, Wang SH, Hou ML, Gu MY, Wang WF. Extraction of mural paint loss diseases based on improved U-Net. Geomat World. 2022;29(01):69–74.
14. Hou M, Zhou P, Lv S, Hu Y, Zhao X, Wu W, Tan L. Virtual restoration of stains on ancient paintings with maximum noise fraction transformation based on the hyperspectral imaging. J Cult Herit. 2018;34:136–44.
15. Guo M, Zhao J, Pan D, Sun M, Zhou Y, Yan B. Normal cloud model theory-based comprehensive fuzzy assessment of wooden pagoda safety. J Cult Herit. 2022;55:1–10.
16. Raviv G, Shapira A, Fishbain B. AHP-based analysis of the risk potential of safety incidents: case study of cranes in the construction industry. Saf Sci. 2017;91:298–309.
17. Zhao J, Tian J, Meng F, Zhang M, Wu Q. Safety assessment method for storage tank farm based on the combination of structure entropy weight method and cloud model. J Loss Prev Process Ind. 2022;75: 104709.
18. Yang Y, Yu B, Tai H, Shen L, Liu F, Wang S. A methodology for weighting indicators of value assessment of historic building using AHP with experts' priorities. J Asian Archit Build Eng. 2022;21(5):1814–29.
19. Guo Y, Tao J, Yang F, Chen C, Reniers G. An evaluation of the information literacy of safety professionals. Saf Sci. 2022;151: 105734.
20. Ben-dong Q, Quan L, Jun-kun T. Construct safety evaluation of the ancient masonry and wood buildings based on fuzzy analytic hierarchy process method. J Civ Eng Manag. 2017;34:52–9.
21. Zhang G, Wang E, Zhang C, Li Z, Wang D. A comprehensive risk assessment method for coal and gas outburst in underground coal mines based on variable weight theory and uncertainty analysis. Process Saf Environ Prot. 2022;167:97–111.
22. Lin C, Zhang M, Zhou Z, Li L, Shi S, Chen Y, Dai W. A new quantitative method for risk assessment of water inrush in karst tunnels based on variable weight function and improved cloud model. Tunn Undergr Space Technol. 2020;95: 103136.
23. Chen Y, Xie S, Tian Z. Risk assessment of buried gas pipelines based on improved cloud-variable weight theory. Reliab Eng Syst Saf. 2022;221: 108374.
24. Xu X, Huang Q, Ren Y, Sun HB. Condition assessment of suspension bridges using local variable weight and normal cloud model. KSCE J Civ Eng. 2018;22:4064–72.
25. Yang J, Tan FH, Tan A, Parke M. Sustainability evaluation of the Great Wall of China using fuzzy set concepts by incorporating leadership energy and environmental design. Civ Eng Environ Syst. 2017;34(1):1–33.
26. Xu S, Ma Q, Xu S. Fuzzy comprehensive evaluation of the compatibility of restoration materials—case study in the rammed earth restoration of the M2 Han tomb in Dingtao, Shandong Province. J Cult Herit. 2022;57:131–41.
27. Dawood T, Elwakil E, Novoa H, Delgado J. Soft computing for modeling pipeline risk index under uncertainty. Eng Fail Anal. 2020;117: 104949.
28. Wu B, Liu P, Huang W, Meng G. Safety assessment of ancient buildings under adjacent subway blasting construction based on the optimized fuzzy optimal method. Shock Vib. 2021;2021(1):2573201.
29. Fu L, Ding M, Zhang Q. Flood risk assessment of urban cultural heritage based on PSR conceptual model with game theory and cloud model—a case study of Nanjing. J Cult Herit. 2022;58:1–11.
30. Li XJ, Wang C, Chen WB, Bora S, Yap JBH, Samuel B. Green building performance assessment in China using a cloud model. Environ Dev Sustain. 2022;24:1–25.

Publisher's Note